

Estimation of uncertainty in thermal environmental projection around Nagoya metropolitan area

HARA, Masayuki^{1*}; ADACHI, Sachiko²; KUSAKA, Hiroyuki³; KIMURA, Fujio⁴; TAKAHASHI, Hiroshi⁵; MA, Xieyao⁴

¹Center for Environmental Science in Saitama, ²Advanced Institute for Computational Science, RIKEN, ³Center for Computational Sciences, University of Tsukuba, ⁴Japan Agency for Marine-Earth Science and Technology, ⁵Tokyo Metropolitan University

Urban canopy process is essential to investigate thermal environment in the near future, because surface air temperature (SAT) increase due to urban heat island is comparable to the one due to the global warming in the near future over major metropolitan areas in Japan. During the past 100 years, annual mean surface air temperature (SAT) increased about 2 °C in Nagoya, while the world mean SAT increased only 0.66 °C. The difference in the SAT is mostly caused by the effect of the urban heat island (UHI). This study investigates the uncertainty in the near future thermal environmental projection of Nagoya metropolitan area which is third largest metropolitan area in Japan. The present climate simulation is conducted using a high-resolution numerical climate model, the Weather Research and Forecasting (WRF) model, including an urban canopy sub-model. A future climate run is conducted using the pseudo-global-warming method, assuming the boundary conditions in the 2050s estimated by CMIP5 GCMs under the RCP scenarios.

Keywords: urban climate, urban heat island, climate projection, dynamical downscaling, regional climate modeling

Development of Urban Meteorological LES Model for thermal environment at city scale

IKEDA, Ryosaku^{1*} ; KUSAKA, Hiroyuki¹

¹Center for Computational Sciences, University of Tsukuba

In this research, a large eddy stimulation (LES) model capable of simulating urban areas was developed, and the degree of impact of buildings, parks, and trees on the local temperature distribution was evaluated.

The main features of the LES model include (i)Building resolving, (ii)Roadside trees are resolved in 3-dimensional, (iii) resolving shadows from buildings and trees, (iv)Multiple reflections of short- and long-wave radiation between buildings and trees by radiosity method, and (v) incorporation of cloud physics and atmospheric radiation models (e.g., RRTM). The radiative environment within an urban canopy layer is an important factor in determining local- or micro-scale temperature distribution. In order to investigate how a 3-D structure (i.e., buildings and trees) can affect the urban thermal environment, we have developed an urban radiation model. Our urban radiation model is able to consider multiple reflections between buildings or trees. Short- and long-wave radiations are calculated by radiosity method. In our tree model, each individual tree is idealized as a porous board constituted by many layers of leaves, and each board is characterized by its Leaf Area Index. The Leaf Area Index is determined by the leaf density of each layer. Optical parameters are leaf transmittance and reflectance. The intensity of direct solar radiation is decreased by passing through the porous boards. Reflected solar radiation is calculated by the radiosity method.

Several model verification tests are performed to evaluate the robustness of model dynamics and physics, and radiation. Based on these numerical test results, our model is correctly developed at least with regarding dynamics, physics, and radiation.

Numerical simulations of thermal environment in Tajimi city, Japan were conducted to perform sensitivity analyses of roadside trees effects, impact evaluations, and future projections of urban thermal environment at city-scale.

Furthermore, we plan to examine how to plan adaptation to urban thermal environmental problems using our LES model.

Keywords: Large Eddy Simulation, Urban Thermal Environment

Development of computational method for micrometeorological field using SGS model based on turbulence structures

INOUE, Minoru^{1*}

¹DPRI, Kyoto University

The diffusion phenomena of heat and pollutants caused by heat convection and turbulent flows in the non-isothermal field is one of the important phenomena concerned with local heavy rain or high levels of air pollution. For example, it can be considered that the heat or the vapor exchange perform actively around the rapidly developed cumulonimbus clouds, or it is said that the circulating flow over an urban area under the heat island phenomenon leads to high concentration of the air pollution. Therefore, it is considered that understanding of those behavior and turbulence structures contributes to a short time prediction of the local heavy rain or a relaxation of the air pollution. And recently, the local heavy rain showing the tendencies to increase occur in the region with horizontal dimensions of a few kilometers and within about 1 hour, they are small scale phenomena both spatially and temporally compared with the heavy rain caused by the typhoon or the movement of the front. The large eddy simulation (LES) which can analyze the turbulence structures in the non-isothermal field is considered as one of the effective means for investigating those phenomena.

The purpose of this study is to develop a computational method for the LES of the turbulent transport of heat and vapor in the micrometeorological field. The governing equations are the continuity equation, Navier-Stokes equations, heat, vapor and liquid water transfer equations, and the condensation process is applied for considering the phase change of water. The governing equations are discretized by the finite volume method in a generalized curvilinear coordinate system so that it can be also applicable to a complex terrain. The coherent-structure Smagorinsky model (CSM) based on the turbulence structures suggested by Kobayashi (2005) is applied as a subgrid-scale (SGS) turbulence model. This turbulence model enables to calculate a suitable model coefficient automatically depending on the turbulent flow field, and is also superior in a numerical stability.

The numerical experiments of turbulent channel flow and back-step flow in the isothermal field were carried out to demonstrate the validity of this turbulence model. The present method was also applied to the LES of the Reyleigh-Bénard convection and the shallow cumulus convection which was similar to the intercomparison study carried out by Siebesma et al. (2003). The computed results showed the good agreements compared with the physical or the other numerical experimental results, so the results suggested the possibility of this method for the analysis of the turbulent transport of heat and vapor.

Keywords: micrometeorology, LES, SGS model, turbulent transport of heat, local heavy rain, air pollution

District scale thermal environment simulations and observations

SUGIYAMA, Tooru^{1*} ; SOGA, Yuuta² ; SADOHARA, Satoru² ; TANAKA, Takahiro³ ; GOTOU, Kouji¹ ;
TAKAHASHI, Keiko¹

¹JAMSTEC, CEIST, ²Yokohama National University, Institute of Urban Innovation, ³Hiroshima University, Graduated School of Engineering

The understanding of these air-thermal and wind conditions in the streets of the well-matured district gets more important because the conditions get worse especially in summer. The reasons for the uncomfortable wind are the complex shape of the building in the districts. The others in the thermal conditions are mainly by the heat-island effects and the global warming in climate change. Indeed, the average temperature in Yokohama-City increases more than that of the global warming. The temperature increase, for example, tends to increase the frequency of a thermal attack to people in the street. The local government officers now try to improve the environment to reduce / decline some kinds of the thermal attacks, then, they demand the information about these thermal and wind conditions.

Here we have performed detailed numerical simulations and observations in order to understand these thermal and wind condition in the streets. The site is Minato-Mirai 21 district (MM21) in Yokohama bay area. The resolutions are 5 meter in space, below 1 second in time. The heat emissions from these air-conditioners, factories, plants, cars, and so on. The land use conditions are also spatially resolved in the calculations. The results are compared with observation results to understand what kinds of the physical processes work there. The pseudo-particle analysis is also performed, then it is frequently observed that the cool air parcels are penetrated into the center of MM21.

These results could bring very useful information to both the local government officers and the stakeholders to improve and design the street environments.

Keywords: Heat environment simulation, particle analysis

Multiscale factors causing climatological high temperature in Tajimi, the 'hottest city' in Japan

TAKANE, Yuya^{1*} ; KUSAKA, Hiroyuki² ; KONDO, Hiroaki¹ ; OKADA, Maki³ ; ABE, Shiori³ ; TAKAKI, Midori³ ; MIYAMOTO, Kenji⁴ ; FUJI, Yukino⁴ ; NAGAI, Toru⁴

¹National Institute of Advanced Industrial Science and Technology, ²Center for Computational Sciences, University of Tsukuba, ³Graduate School of Life and Environmental Sciences, University of Tsukuba, ⁴Tajimi City Government

In this study, multiscale climatological features of extreme high temperature (EHT) events in Japan's hottest city, Tajimi in Gifu Prefecture were investigated using observational data corrected by Japan Meteorological Agency (JMA) during past 23 years and original data observed by authors during three years. The results showed that the occurrence of a specific pressure pattern of 'WHALE' (tail of a whale) — the synoptic-scale factor — and the urbanisation of Tajimi (meso γ scale) are the background factors that lead to climatologically high temperatures in Tajimi. In addition, the high-temperatures in Tajimi are contributed by the foehn-like westerly airflow coming from the mountains located in the northwest/western side, which cover the inland part of the Nobi Plain (the meso β scale factor), and the location of Tajimi observation station established within the urban section (~about 400 m²) of the city where high temperatures tend to be observed (the microscale factor). On the other hand, statistical analysis indicated the possibility that the small-scale basin effects and soil dryness around Tajimi City (the meso γ scale factors), which were proposed as other hypotheses, do not play a climatological role in the occurrence of the EHT events in Tajimi.

Keywords: Extreme high temperature, Pressure pattern, Foehn, AMeDAS, Tajimi

Lidar development for hyper-dense remote observation of urban atmosphere

ABO, Makoto^{1*} ; KIKUTA, Tatsuya¹ ; ARUGA, Kouki¹ ; PHAM LE HOAI, Phong¹

¹Tokyo Metropolitan University

Information of atmospheric temperature and water vapor density are most important factor for the prediction of air pollution, an analysis of the nature of the heat island phenomenon and the prediction of localized heavy rain in urban area. We are developing practical instruments for remote measurements of atmospheric temperature and water vapor density distributions with sub-kilometer range resolution.

For water vapor concentration distribution measurement, we propose a differential absorption lidar (DIAL) using diode laser based transmitters. For temperature measurements in daytime, we propose a high-spectral-resolution lidar (HSRL) using a potassium Faraday filter. The Faraday filter acts as a blocking filter for suppression of narrow Mie scattering, and a very narrow filter for getting temperature information from Doppler-broadened Rayleigh spectrum.

Keywords: hyper-dense observation, lidar, atmospheric temperature, water vapor density, remote sensing

Geographical distribution of outgoing thermal radiation intensity in downtown Tokyo on hot days and mitigation measures

TSUNEMATSU, Nobumitsu^{1*} ; YOKOYAMA, Hitoshi¹ ; HONJO, Tsuyoshi² ; ICHIHASHI, Arata¹ ; ANDO, Haruo¹ ; MATSUMOTO, Futoshi¹ ; SETO, Yoshihito³ ; SHIGYO, Nobuhiko²

¹Tokyo Metropolitan Research Institute for Environmental Protection, ²Chiba University, ³Tokyo Metropolitan Research Institute for Environmental Protection/Tokyo Metropolitan University

Annual mean air temperatures in downtown Tokyo have increased about 3 degrees Celsius in the past 100 years due to global warming and urban heat island (UHI) (Japan Meteorological Agency, 2014). Also, the frequency of heat stroke outbreaks tends to increase. These promote implementation of measures for summer heat in Tokyo. We have investigated the impacts of UHI mitigation and adaptation strategies such as making highly reflective pavements, creating green and water spaces, etc.

As part of the investigations, we analyzed data from thermal infrared (TIR) remote sensing in downtown Tokyo on four different extremely hot days: Aug. 7, 2007, Aug. 10, 2007, Aug. 19, 2013, and Aug. 19, 2014. The TIR measurements were carried out in the daytime (12-13 local time: LT) and the nighttime (around 21 LT) (except for Aug. 10, 2007) under similar weather conditions, using a long-wave infrared (8-14 um wavelength) camera (NEC Avio; TS7302) installed on a helicopter. The helicopter was flying at Flight Level 20 (2,000 ft, i.e., 610 m). The lower flight level allows horizontal spatial resolution of data from the thermal imaging camera to be significantly high (approximately 2 m) in spite of airborne TIR measurements. Although sea breezes prevailed over downtown Tokyo, daily maximum air temperatures on those days reached around 34 degrees Celsius.

Areas for the airborne measurements on Aug. 19, 2013 and Aug. 7, 2007 include "Ochanomizu", "Marunouchi", "Otemachi", and "Ginza". To verify impacts of recent UHI mitigation and adaptation strategies in those cities, we analyzed changes in the surface infrared radiation intensities (outgoing longwave thermal radiation intensities) between 2007 and 2013. Surface infrared radiation intensity is one of the important factors that strongly affect sensible temperatures. Compared with other factors affecting sensible temperatures, surface infrared radiation can be easily controlled by UHI mitigation and adaptation strategies for lowering surface temperatures without the negative influences on other places, i.e., no trade-off relationship between changes in the radiation intensities (surface temperatures) at a specific place and another place.

The results show that daytime surface infrared radiation intensities in 2013 are relatively high in the greater part of the area, compared with the ones in 2007, owing to extremely hot weather conditions in 2013, nevertheless, lower intensities of surface infrared radiation can be recognized in some redevelopment areas where several new buildings were constructed between 2007 and 2013. This appears to be due to green and water spaces created in the redevelopment areas through the UHI mitigation and adaptation strategies. Incidentally, surface infrared radiation intensity changes between 2007 and 2014 in the "Shinjuku" city and the neighboring areas will also be analyzed.

By using the TIR remote sensing data, we picked out hot spots where mitigation and adaptation strategies for lowering surface temperatures should be required. For instance, the daytime TIR images superimposed on GIS (geographic information system) applications showed higher infrared radiation intensities (higher temperatures) on surfaces of intersections and the northern parts of streets running from east to west. To clarify the causes of those hot spots, we investigate relationships among surface infrared radiation intensities (surface temperatures), sky view factors, etc. Also, we analyze thermal environment around venues of the 2020 Summer Olympic and Paralympic Games.

Acknowledgements: We are grateful to Ms. Masami Hori, Bureau of Environment of Tokyo Metropolitan Government. She provided us with helpful data as to the UHI mitigation and adaptation strategies.

Keywords: urban heat island, downtown Tokyo, surface infrared radiation intensity, mitigation and adaptation strategies, airborne remote sensing, GIS applications

The horizontal distance of each cumulus and broadening distance of stratiform clouds determines shallow cloud cover

SATO, Yousuke^{1*} ; NISHIZAWA, Seiya¹ ; YASHIRO, Hisashi¹ ; MIYAMOTO, Yoshiaki¹ ; KAJIKAWA, Yoshiyuki¹ ; YOSHIDA, Ryuji¹ ; YAMAURA, Tsuyoshi¹ ; TOMITA, Hirofumi¹

¹RIKEN, Advanced Institute for Computational Science

Shallow cloud cover below sharp inversion is determined by the relationship between two scales. One is the horizontal distance of each cumulus and the other is the horizontal broadening distance of the stratiform clouds at the top of the boundary layer. We indicated it through the numerical experiments of a transition from cumulus under stratocumulus to the shallow cumulus off the west coast of California. The experiments were conducted with an extremely wide domain (i.e. 300 km × 28 km) using a large eddy simulation model with fine grid resolution (i.e. $dx = dy = 50\text{m}$, $dz = 5\text{m}$). The results show that cloud cover is high with large broadening distance of the stratiform clouds and a short distance between each cumulus. In contrast, low cloud cover occurs when the broadening distance is smaller than the distance of each cumulus. The contrast of the two distances is generated by the difference in aerosol the amount and the strength of surface heat flux. The small broadening distance of the stratiform clouds occurs when the surface heat flux (the aerosol amount) is strong (small), and vice versa. The effects of the surface heat flux are larger than that of aerosol amount.

The relationship between two distances can be applied for estimating the cloud cover below the sharp inversion. Hence, it is of help for improving the better expression of shallow clouds in global scale model.

Keywords: Large Eddy Simulation, Stratocumulus, Cumulus, Cloud Cover

Analysis of particulate Bragg scattering due to turbulent clustering in cumuli based on direct numerical simulations

MATSUDA, Keigo^{1*} ; ONISHI, Ryo¹ ; TAKAHASHI, Keiko¹

¹JAMSTEC

Radar observation is one of powerful tools to obtain data regarding the cloud physics. The radar observation data are analyzed based on the relation between the radar reflectivity factor and the cloud physical properties. In most cases, the relation derived assuming homogeneity and randomness of particle distributions is used. However, spatial correlations of cloud droplets cause particulate Bragg scattering, which increases the reflected microwave intensity in radar observations. The particulate Bragg scattering is assumed to be insignificant in clouds for a long time. However, the particulate Bragg scattering can be significant due to cloud turbulence. One of the turbulence effects in clouds is turbulent droplet clustering: cloud turbulence generates microscale clusters of cloud droplets due to centrifugal effects. The authors' group performed a three-dimensional direct numerical simulation (DNS) of particle-laden isotropic turbulence and revealed that the influence of turbulent clustering can be a cause of significant error in radar observation of clouds (Matsuda et al., J. Atmos. Sci., 2014). The DNS was performed under the conditions with monodispersed droplets: all droplets in a domain have the same size. This study aims to investigate the influence of turbulent clustering on the radar reflectivity factor for the case of polydispersed cloud droplets; i.e., droplet size distribution in cumulus clouds are considered in the DNS. In the DNS, an isotropic turbulence is generated by solving the Navier-Stokes equation without any turbulence model and a large number of droplet motions are tracked by the Lagrangian method. The clustering data are used to calculate the intensity of scattering microwave considering particulate Bragg scattering. The radar reflectivity factor is calculated from the scattering intensity. We will show the results of the radar reflectivity factor analysis comparing with the factor based on the turbulent clustering data for monodispersed droplets, and discuss the influence of turbulent clustering on radar cloud observations.

Keywords: direct numerical simulation, turbulent clustering, radar reflectivity factor

Development of the C-band radar system with the good temporal and spatial resolutions

FURUMOTO, Jun-ichi^{1*} ; MATSUDA, Tomoya² ; KAKIMOTO, Ikuya² ; HIGASHI, Kuniaki¹

¹Research Institute for Sustainable Humanosphere, Kyoto University, ²Mitsubishi Electric Corporation

The C-band weather radar has an advantage in detecting the precipitation echo without the attenuation effects by precipitation particle in the long distance. Recently, the active phased array system is implemented to the X-band weather radar, which enables all-sky scan within a minutes. However, it is difficult to develop the phased array system for C-band weather radar, because of the large antenna size. This paper introduce our project to develop the new C-band radar system with the good temporal and spatial resolutions. The super-resolution technique such as the radar imaging is also discussed in this paper.

Keywords: C-band weather radar, radar imaging, high temporal and spatial resolutions

Numerical Simulation on Development Process of a Cb in the Early Developing Stage observed by Ka-band and X-band radars

SAKURAI, Namiko^{1*} ; SHIMIZU, Shingo¹ ; MISUMI, Ryohei¹ ; IWANAMI, Koyuru¹

¹NIED

Millimeter-wavelength radar is a useful tool for observing the initiation and early developing stage (DS) of cumulonimbi because it has higher sensitivity and higher spatial resolution than those of conventional weather radars (S-, C-, and X-band radars; centimeter-wavelength radars). The National Research Institute for Earth Science and Disaster Prevention (NIED) of Japan has a Ka-band Doppler radar (KaDR) with mobile capability (Iwanami et al., 2001) and performed intensive observation of cumulonimbi with the KaDR and an X-band polarimetric Doppler radar (MP-X) in the western Kanto region, Japan during the summer of 2011-2013. Sakurai et al. (2012) successfully observed a cloud from initiation to the DS using the KaDR and from the DS to the dissipation stage using the MP-X on 18 August 2011, and revealed that the echo top height which developed stepwise corresponded to the height of three stable layers in the atmosphere. It is considered that the following convective activity broke through the stable layers in the DS, and echo top height finally reached 12 km ASL.

To clarify the development mechanism of the cumulonimbi, we performed numerical simulations using a CReSS, which is a 3D non-hydrostatic model developed by the Hydrospheric Atmospheric Research Center (HyARC) of Nagoya University, Japan (Tsuboki and Sakakibara, 2002). We used sounding data at Tateno at 09 JST (JST = UTC + 9 hr) on 18 August 2011 for the initial and lateral boundary conditions. We ran an experiment that positive perturbation (about 2 K) was added intermittently with an interval of 15 minutes as a buoyancy forcing at a height of 500 m around initiation region of the convection observed by the KaDR. The numerical simulation successfully reproduced the stepwise development of the cumulonimbus. In the beginning of the DS, convection was shallow for about an hour and the convection developed gradually. The development of the convection was suppressed around stable layers. The latter convection developed deeper than the former one, which was also consistent with observational result. From the investigation on temporal variation of RH profiles in the numerical simulation, preceding convection could not break through the low-level stable layers, however it moistened the lower troposphere. It is considered that the following convection could break through the stable layers because it could possess positive buoyancy enough to break through the stable layers due to low entrainment rate in the moistened lower troposphere.

Keywords: Cumulonimbus(Cb), Numerical Simulation, Ka-band radar

A novel measurement system for thermodynamic environment by using radio astronomy technology

TAJIMA, Osamu^{1*} ; NAGASAKI, Taketo¹ ; KOMINAMI, Kinichiro² ; ARAKI, Kentaro³

¹High Energy Accelerator Research Organization, Institute of Particle and Nuclear Studies, ²Nomura Securities Co., Ltd.,
³Meteorological Research Institute, Forecast research department

In order to prevent meteorological disasters such as local heavy rainfall, significant tornado, and heavy snowfall, a novel method of short-term forecasting and nowcasting is required. To solve this issue, we propose a novel measurement system which high-frequently observes microwave radiation intensity and estimates atmospheric thermodynamic environment.

We have been developed such a radiometric measurement system based on the technology for the radio astronomy. There are absorption characteristics by water vapor and liquid water at the frequency of 20-30 GHz. The radiometric observation at these frequencies has been used for the retrieval of vertically integrated water vapor and liquid water. Recent studies have applied the radiometric observations at another frequency band of Oxygen molecule absorption (50-60 GHz) to the retrieval of vertical thermodynamic profiles such as atmospheric temperature and water vapor. A key to achieve a high-quality and high-frequently radiometric observation is maintenance of cold condition, e.g., 20 Kelvin, for a cold amplifier. It results in low noise condition of the radiometer. Application of the radio astronomy technology naturally achieves this because cooling of the receiver is the popular technique. In particular, mechanical refrigerator on the high-speed rotation system, which is the patent pending technology by authors, realizes the high-speed scan of the sky.

We will present an outline of this project as well as status of its prototype system at 22 GHz band. The plan for 3-dimensional mapping of the atmospheric water vapor and for retrieval of cloud microphysics properties such as snow water path will be discussed, too.

This research is funded by "Program for Creating STart-ups from Advance Research and Technology (START Program)" from the Ministry of Education, Culture, Sports, Science and Technology, Japan, <http://www.jst.go.jp/start/en/index.html>.

Keywords: atmospheric water vapor, radiometer, thermodynamic environment

Microwave Radiometer Network (Micro-NET) in Kanto region for high-temporal monitoring of vapor

SHIMIZU, Shingo^{1*} ; IWANAMI, Koyuru¹ ; MAESAKA, Takeshi¹ ; KIEDA, Kaori¹ ; NAKAI, Sento¹ ;
HONDA, Meiji²

¹NIED, ²Niigata univ.

National Research Institute for Disaster Prevention (NIED) had developed microwave radiometer network (Micro-NET) in Kanto region since 2014. The Micro-NET will provide vertical profile of vapor and temperature in high temporal resolution and contribute as a powerful tool for data assimilation to improve forecast skill of early developing cumulonimbus. NIED installed another three microwave radiometers (MWR) in Niigata prefecture to retrieve temperature profile in snow storms.

This study will report the preliminary results on the performance of MWRs by the comparison between MWR and sounding data at Tsukuba and Niigata cite.

Keywords: Microwave radiometer, vapor

Doppler radar and lidar analysis for 13 June 2014 Fuchu City hailstorm using a 3DVAR

SHIMOSE, Kenichi^{1*} ; SHIMIZU, Shingo¹ ; SUZUKI, Shin-ichi¹ ; SHUSSE, Yukari¹ ; MAESAKA, Takeshi¹ ;
KIEDA, Kaori¹ ; IWANAMI, Koyuru¹

¹National Research Institute for Earth Science and Disaster Prevention

This paper is described about a 3DVAR analysis of the hailstorm event on 13 June 2014 around Fuchu City, the Tokyo Metropolitan Area, Japan. The hail with a diameter of 3 centimeters and wind gust were reported with this event. This hailstorm was observed by multiple X-band polarimetric Doppler radar and a Doppler lidar, simultaneously. For this case, the CReSS 3DVAR with MSM for a background field was used to analyze the wind structure of this hailstorm.

On that day, there was a cold low in the northern part of Japan and a trough was laid on the Tokyo Metropolitan Area. The duration of the hailstorm is about 3.5 hours (from 1000 LST to 1330 LST), and hail fell around 1210 LST. The analysis of the X-band polarimetric Doppler radar shows that the region of hail was located the southern edge of the storm and was indicated large specific differential phase (Kdp) value (8 degree km⁻¹) at 1 km AGL. This large Kdp region also corresponded to strong downdraft region (5 m s⁻¹) at 1 km AGL. The reported wind gust might be caused by this strong downdraft. The Doppler lidar, which was located on the warm sector of the hailstorm, completely succeeded to capture the radial velocity of the inflow toward the hailstorm.

The 3DVAR analysis of horizontal wind field at 500 m AGL shows that the horizontal wind field is greatly improved the flows into the hailstorm around the observation range of the Doppler lidar. The 3DVAR analysis also improve the flows out to the hailstorm around the observation range of the X-band polarimetric Doppler radar, and the boundary of the outflow and inflow of the hailstorm is clearly analyzed. For a future work, it is planned to carry out the prediction experiment of the hailstorm using the analyzed fields.

Keywords: Doppler radar, Doppler lidar, hail, data assimilation

30-second-update ensemble Kalman filter experiments using JMA-NHM at a 100-m resolution

KUNII, Masaru^{1*} ; RUIZ, Juan² ; LIEN, Guo-yuan³ ; USHIO, Tomoo⁴ ; SATOH, Shinsuke⁵ ; BESSHO, Kotaro⁶ ; SEKO, Hiromu¹ ; MIYOSHI, Takemasa³

¹Meteorological Research Institute, ²University of Buenos Aires, ³RIKEN Advanced Institute for Computational Science, ⁴Osaka University, ⁵National Institute of Information and Communications Technology, ⁶Meteorological Satellite Center

Local severe rainstorms may cause serious damage such as flooding and landslide, but its precise simulation is difficult mainly due to limited spatial and temporal resolutions of numerical weather prediction (NWP). To tackle this challenge, a 100-m-resolution NWP system is designed, so that the forecasts are updated every 30 seconds by assimilating observational data from the phased array weather radars (PAWR) at Osaka and Kobe. In addition, the next-generation geostationary satellite Himawari-8 will have a 30-second scanning mode for a limited domain, and using the Himawari-8 data is within the scope. An observation operator and quality control algorithm are developed for PAWR, and data assimilation experiments using the Local Ensemble Transform Kalman Filter (LETKF) are performed for the local heavy rainfall case that caused a disaster in Kyoto on 13 July 2013. In this presentation, a brief introduction to the experiments and the results will be presented.

Keywords: data assimilation, ensemble Kalman filter, phased array weather radar

Numerical Simulation of Heavy Snowfall and the Potential Role of Ice Nuclei in Cloud Formation and Precipitation

ARAKI, Kentaro^{1*} ; MURAKAMI, Masataka¹ ; TAJIRI, Takuya¹ ; SAITO, Atsushi¹ ; SHOJI, Yoshinori¹

¹Meteorological Research Institute, JMA

A heavy snowfall event occurred in the Kanto and Koshin regions from 14 to 15 February 2014, when a winter extratropical cyclone rapidly developed along the south coast of Japan. The snow cover exceeded the historical record in these regions. In order to examine the characteristics of cloud microphysics during the event, we performed a numerical simulation with a horizontal grid spacing 1.5 km and a model domain covering the Kanto and Koshin regions by the JMA Non Hydrostatic Model (JMA-NHM) with bulk-type cloud microphysics. The initial and boundary conditions were provided from 3-hourly JMA mesoscale analyses. The precipitating clouds and atmospheric conditions were simulated for 33 hours from 03 Japan Standard Time (JST) on 14 February 2014.

From the result of high-dense snow cover observations, the total snowfall exceeded 1 m in the areas along the mountains in the Yamagashi, Gunma, and Tochigi prefectures during the event. The numerical simulation successfully reproduced the distribution of total snowfall. By comparing the result of the simulation with the surface observations of automatic weather stations in Tokyo metropolitan, temporal variations of simulated surface atmospheric temperature and relative humidity were consistent. In order to evaluate the reproducibility of cloud microphysics in simulated precipitating clouds, the ground-based microwave radiometer (MWR) operated in the Ome city in Tokyo metropolitan was used in this study. Liquid water path (LWP), which is retrieved from radiometric observations by a statistic inversion method, is compared with simulated LWP during the event. The data including errors due to rain was excluded from the comparison, so that there is large difference between precipitable water vapor (PWV) retrieved by radiometric observations and PWV derived from the global positioning system. As the result, temporal variation of simulated LWP was similar to that of retrieved LWP.

Clouds composed of cloud ice were simulated at the altitude 8-12 and 2-4 km above the Ome city, and the latter cloud was formed on the boundary of a coastal front. Mixing ratio of snow was large below the altitude of 6 km, and number concentration of snow was large at the altitude of 4-10 and 1-3 km. In this case, there were two layers of ice clouds and the heavy snowfall would be increased due to the seeder-feeder effect. Total precipitation by graupel reached 30 mm in some parts of the Kanto region, which was formed by riming process during the passage of the extratropical cyclone in the Kanto plain, where sufficient water vapor flux and super-cooled cloud water existed in low-level troposphere.

In order to investigate the effect of ice nuclei on snowfall, sensitivity experiments were performed by changing coefficients of 0.1 (IN01) and 10 (IN10) times in the formulas of ice nucleation (Meyers 1992) and freezing (Bigg 1955) in JMA-NHM. As the result, there were differences of total precipitation by snow of -5 mm in IN01 and +2-+5 mm in IN10 from the control experiment in the areas with large amount of total snowfall. This difference would be caused by the change of snow due to the change of ice number concentration where there was sufficient water vapor flux below the altitude about 5 km. The total precipitation by rain increased more than 15 mm in IN01, and also decreased less than 20 mm in IN10 in the Kanto plain. On the other hand, total precipitation by graupel decreased about 5 mm in IN01 and increased over 10 mm in IN10 in the areas including the Tokyo metropolitan and Saitama prefecture. Since there were sufficient middle-level snow, low-level water vapor flux, and super-cooled cloud water in the windward side of these regions, snow falling from the upper ice cloud was converted to graupel in the low troposphere in IN10. These results suggest that there are uncertainties related to the aerosol indirect effects in cloud microphysics modeling of bulk method in JMA-NHM.

Keywords: heavy snowfall, numerical simulation, cloud microphysics, ice nuclei

The analysis of the relation between non-precipitation echoes and wind structure of sea breeze

NAGUMO, Nobuhiro^{1*} ; KATO, Teruyuki¹

¹Meteorological Research Institute

Local severe weathers by isolated cumulonimbus cloud occasionally occurs in summer of Kanto Plain. One of the trigger is known to be a local circulation as a sea breeze front. The local circulation structure under no precipitation condition cannot be detected by operational radar and ground observation network as AMeDAS, however, non-precipitation echoes are occasionally observed in fine day or around area of heavy rain in rainy day. The case on July 23, 2013 was representative of non-precipitation echoes prior to the local heavy rain. The Doppler Radar for Airport Weather (DRAW: 60 km in observation radius) set at Haneda detected the behavior of non-precipitation echoes which showed convergence near coast line and moved toward inland several hours before cumulonimbus generations. Finally heavy rain occurred near the non-precipitation echoes convergence line. This fact suggested that the non-precipitation echoes have a relation with sea breeze structure. To clarify the detail relations between non-precipitation echoes and sea breeze as generation source and distribution of the echoes, we analyzed the dense network observation data consisting of Doppler lidar (6 km in observation radius) and surface observation system with operational observation network of DRAW. The Doppler lidar was installed at Tokyo Institute of Technology in Ookayama, which is 10 km northwest of DRAW at Haneda. This lidar succeeded in observing air structure around sea breeze front and made possible the complex observation with DRAW. Furthermore, we performed the high-resolution simulation (250 m) of JMA-NHM (Non-Hydrostatic Model of Japan Meteorological Agency) to discuss the generation and distribution of non-precipitation echoes.

Doppler lidar image (SN ratio/Doppler Velocity) depicted the sea breeze structure with landward lower flow and counter current above. The sea breeze thickness was about 1500 m at maximum and had Lobes and Cleft structures. In the lidar detectable range, two Lobe-like shapes and one gap (Cleft) between two Lobes were observed. Next, non-precipitation echoes observed by DRAW were shown rather several kilometers seaward (leeward) from the sea breeze front observed by the lidar. The distribution of non-precipitation echoes also showed vertical direction of perturbations with its flow and the echo convergence line showed gradual approach toward sea breeze front. Additionally, The non-precipitation echoes exhibited interesting relations with the sea breeze structure. In the rear of Lobes and thin Cleft structures, non-precipitation echoes distributed at lower altitudes near surface (~200 m) and in front of the Lobe structures was higher altitudes (~800 m) and convergence were detected around Cleft structures (front of Lobe - Cleft).

JMA-NHM simulation of 250 m resolution represented the above-mentioned wind structure well. The front of Lobe showed upward flow and the rear showed down flow. Surface convergence was simulated around Cleft structures. The up- and downward wind exhibited the horizontal circulation in Lobe structures.

In this presentation, we will show the results of observation (e.g., Lobes and Cleft structure, convergence of echoes, and vertical perturbations of echoes) and the discussion results about the relation between non-precipitation echoes distribution and wind structures focusing on pressure perturbation and thermal/mechanical structures.

Keywords: Local circulation, Dense observation (Radar/Lidar), Numerical Simulation

Elucidation of the mechanism of the downstream gust wind using high resolution weather model

HIGASHI, Kuniaki^{1*} ; FURUMOTO, Jun-ichi¹ ; SAKAMOTO, Hiroto¹

¹Research Institute for Sustainable Humanosphere, Kyoto University

This study aims to elucidate the mechanism of the downstream gust-wind blowing from the Hira mountain range to the Lake Biwa in the 10 km-range by using 200 m horizontal-resolution dense non-hydrostatic forecast model. The results of dense in-situ measurement clearly shows this gust wind, called as Hira Oroshi (HO), has very unique characteristics that the location and of gust and period of gust wind varies in each case. Considering that this complex feature of HO has not fully elucidated, this study conducted a long-term simulation in the HO region during October, 2013 and March, 2014. In-situ measurement detected 17 HO event, which is also successfully reproduced by the results of our simulation. The common line shape structure, which causes the gust wind in the West coastline of Lake Biwa, is clarified.

Keywords: downslope wind, gust wind, microscale weather, atmospheric boundary layer, weather simulation

Verification of Off-Zenith Observations by Ground-Based Microwave Radiometer under Stratiform Precipitation Conditions

ARAKI, Kentaro^{1*} ; MURAKAMI, Masataka¹ ; ISHIMOTO, Hiroshi¹ ; TAJIRI, Takuya¹ ; SHOJI, Yoshinori¹ ; SAITO, Atsushi¹

¹Meteorological Research Institute, JMA

The radiometric observation by ground-based microwave radiometer (MWR) has been used for the retrieval of precipitable water vapor (PWV) and liquid water path (LWP) for many decades. However, raindrops cause mainly two critical errors in radiometry; the first is the effect that raindrops wet the radome, which produces absorption losses. The second is the effect of absorption/emission and scattering by large raindrops in the air.

To solve especially the first issue, the effectivity of off-zenith radiometric observations by MWR under the stratiform precipitation conditions in all seasons is investigated. Stratiform precipitation periods were extracted by using the criteria of rainfall rate (RR) observed by an optical disdrometer and LWP retrieved from off-zenith observations at the elevation angle of 15 degrees. By comparing PWVs derived from radiometric observations at the elevation angle of 15 degrees with PWVs derived from global positioning system, it's found that the reliable PWVs are obtained under the stratiform precipitation conditions with RR less than 10 mm h^{-1} . The precipitation particles are mostly classified into snow and graupel at RR over 7 mm h^{-1} , and the particle type of rain is found at small RR. A case study shows that microwave radiometry can be conducted with small errors under the stratiform snow conditions even with RR over 10 mm h^{-1} . By solving a simplified radiative transfer equation applied to the typical stratiform rain cases with small RRs, it's found that the observations at the elevation angles over 30 degrees are affected by the effect of the wetness on the radome. From the result of the fundamental experiments which estimates the errors quantitatively, the errors in zenith observations in the cases are comparable to the error due to the wetness on the radome. The off-zenith observations at low elevation angle are valuable under the stratiform precipitation conditions when the Rayleigh approximation assumed in the retrieval method is appropriate.

Keywords: microwave radiometer, stratiform precipitation, precipitable water vapor, liquid water path, retrieval

Comparison of Tipping-Bucket Rain Gauges in Natural Rainfall Conditions

NAGASE, Tsukasa^{1*}; HAYASHI, Taiichi²; KOMATSU, Ryosuke³; WATANABE, Yoshihiro¹; HASHINAMI, Shinji¹; YAMAMOTO, Akira⁴

¹Weather Information & Communications Service LTD., ²Disaster Prevention Research Institute, Kyoto University, ³Komatsu Factory Co. LTD., ⁴Meteorological Research Institute, Japan Meteorological Agency

On August 2014 three-hour rainfall amount exceeded 200 mm in Hiroshima City, which raised serious damage and loss of life by landslides and debris flows. High-resolution rapid-scan weather radar monitoring systems are obviously effective to mitigate damage by such sediment disaster induced by heavy rain. Radar-estimated rainfall rate has been calibrated by tipping-bucket rain gauges(TBRs) measurement, but there are few comparison studies between radar and TBRs at very high rainfall rate because of localness and scarceness of heavy rain phenomena. Furthermore, accuracy of most of TBRs installed in Japan and Asian rain countries are not guaranteed over 100 mm rainfall rate.

To make sure validity of rainfall rate measured by typical TBRs at high rainfall rate, two field comparisons were carried out in Japan and India. Three resolution types of TBRs, 1.0-, 0.5- and 0.2-mm, were tested at Shionomisaki, Japan and at Cherrapunji in Indian state of Meghalaya, which holds world records of maximum rainfall amount for a month and a year. About 4-month measurement beginning on June 16, 2013 at Shionomisaki and beginning on April 28, 2014 in Cherrapunji were done.

Accumulated rainfall measured by the three different resolution TBRs for the comparison period were 1258.0 mm for 1.0-mm resolution type, 1244.5 mm for 0.5-mm type, and 1209.4 mm for 0.2-mm type at Shionomisaki, while those were 8643.0 mm, 8379.5 mm and 8154.0 mm, respectively at Cherrapunji. It means 1 and 4 percent deficit of rainfall amount measured by 0.5-mm and 0.2-mm resolution TBRs compared to 1.0-mm TBRs at Shimonoseki, and 3 and 6 percent deficit at Cherrapunji, which implies higher resolution TBRs measure less rainfall amount than lower ones.

Frequency of 80 mm/h or higher rainfall intensity estimated by tipping rate of the 1.0 mm TBR were 5 percent (72 cases) at Shimonoseki and 14 percent (1249 cases) at Cherrapunji, while cases of 200 mm/h or higher intensity were 3 and 15, respectively. Maximum rainfall intensity at Shionomisaki was 225mm/h and that at Cherrapunji was 300mm/h.

0.2-mm resolution TBRs measure 1.0 mm rainfall intensity by five tippings, however, number of tippings for 1.0 mm rainfall at higher intensity than 80 mm/h were frequently less than five, which means underestimation for heavy rain. Similarly 0.5-mm TBRs measure 1.0 mm rainfall intensity by two tippings and showed no underestimation for rainfall intensity ranging from 80 mm/h to 200 mm/h. But there were some underestimated cases for higher intensity than 200 mm/h.

In conclusion we found higher resolution TBRs underestimated at higher rainfall intensity than 80 mm/h in two field comparisons. Lower resolution TBRs are recommended to measure rainfall accurately at locations where heavy rain is possible.

Keywords: tipping-bucket rain gauges, local heavy rain, meteorological observation, India

Surface Pressure Distributions of Downburst captured by High Dense Ground Observation Network "POTEKA" on 22 August 2014

SATO, Kae^{1*} ; YADA, Takuya¹ ; KURE, Hirotaka¹ ; KOBAYASHI, Humiaki²

¹Meisei Electric Co. Ltd., ²National Defense Academy

Meisei developed low-cost compact weather sensor (POTEKA Sta., hereinafter referred to as the POTEKA), which can measure temperature, relative humidity, pressure, sunlight, and rain detection per one minute and we installed high ground observation network (total 55 stations, 1.5~4km-mesh) in Gunma in FY2013. The following year, we further improved POTEKA to observe wind direction, wind speed and rainfall. Additionally, we added 93 locations, about 2km intervals, around the elementary school in order to achieve higher density than the existing observation network. Therefore, we can obtain real-time meteorological information per one minute in total 145 stations. This paper presents observation of downburst around Takasaki city and Maebashi city on 22 August 2014.

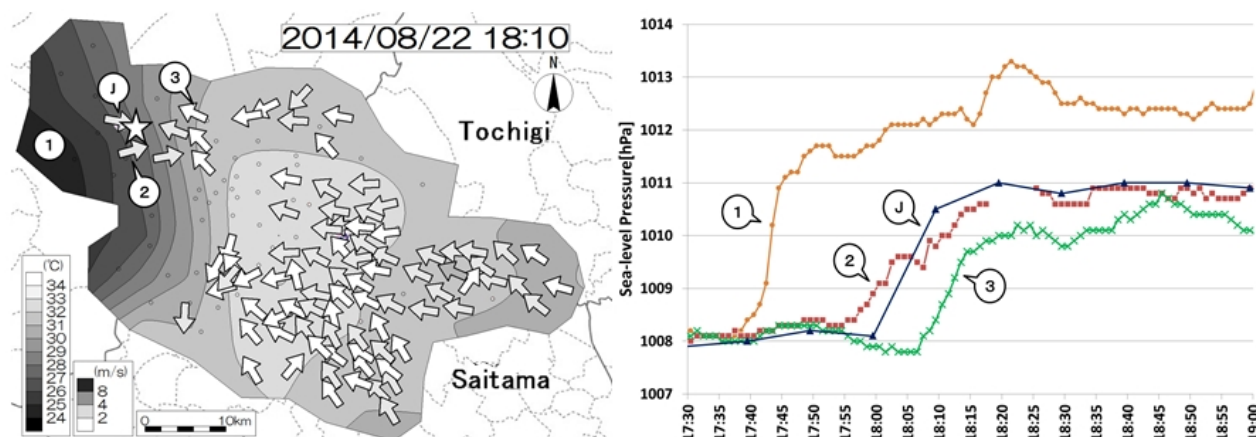
Downburst, accompanied with well-developed cumulonimbus, occurred and passed from Takasaki city to Maebashi city around 18:10. A significant drop in temperature is noticed around 17:45, (-0.47 °C per one minute on average). The distributions and occurrence time of cold air captured by POTEKA network well coincide with field survey results of the Japan Meteorological Agency. In addition, the first temperature drop was confirmed about 25 minutes before damage occurrence time of the downburst. Pressure jumps of 1-2 hPa were recorded at the same time as the temperature drop, and the average increase rate was +0.34hPa per minute. The pressure jump is regarded as a cool and high dense downdraft under the thunderstorms.

In comparison with the case of downburst on 11 August 2013 (Sato et al. 2014, Norose et al. 2014), the temperature decrease rate at last time and at this time are the average -1.15 °C and -0.47 °C per minute, the last case is 2 times larger than this time. Both sudden drops in temperature can be captured by POTEKA in advance to the occurrence of downburst hazard. Furthermore, such pressure jumps were recorded in both 2013 and 2014. But the surface pressure after the occurrence of downburst is maintained at the higher level than the pre-occurrence of downburst in 2014. Several downbursts seem to be continuously generated by the larger and more active cumulonimbus in 2014 than these of 2013, which produced the strong winds and kept the surface high pressure after the first downburst occurrence. We are going to further investigate the surface characteristics during downburst by using other meteorological elements (relative humidity, wind velocity, and etc.).

References

1. Sato K, Kure H, Yada T, Maeda R, Kojima H, Morita T, Iwasaki T. 2014: Surface and Pressure Distributions of Downburst captured by the surface dense observation network POTEKA(1). Meteor. Soc. Japan. 2014 Spring Meeting. 105. 223pp. (in Japanese)
2. Norose K, Kobayashi K, Kure H, Morita T. 2014: Surface and Pressure Distributions of Downburst captured by the surface dense observation network POTEKA(2). Meteor. Soc. Japan. 2014 Spring Meeting. 105. 224pp. (in Japanese)

Keywords: High Dence observation network, Downburst



A Study on the development of forecast system for the downstream wind by Hira Oroshi

SAKAMOTO, Hiroto^{1*} ; HIGASHI, Kuniaki¹ ; FURUMOTO, Jun-ichi¹ ; HASHIGUCHI, Hiroyuki¹

¹Research Institute for Sustainable Humanosphere, Kyoto University

This study aims to develop the precise forecast system of “Hira Oroshi” (hereafter, called as HO), the downstream gust wind blowing down from the Hira mountain range to the West coast of Biwa Lake in Shiga prefecture, Japan. Our system improved the forecast score of gust occurrence to about 80% from 50%.

In this study, the occurrence of downstream gust wind in HO region is defined as the maximum wind speed exceeds to 20 m/s with the wind direction of WEW-NNE.

The intensive observation network was constructed to monitor the detailed behavior of downstream gust and selected four observation points, which can represent the wind field in the whole HO region.

The non-hydrostatic meteorological forecast system with the horizontal resolution of 200 m is constructed by installing WRF (Weather Research and Forecast) to the A-KDK system in Kyoto University. The initial and boundary data is automatically obtained from JMA and other meteorological agencies every six hours. A long-term computational experiment from October 1, 2013 to March 31, 2014 shows very interesting characteristics of wind speed pattern, which appears, only when the gust wind was actually observed.

Narrow strong wind regions extending from the Lake Biwa toward the foot of Hira Mountain range appears and extends to the land in HO region. This structure is used to identify the appearance of gust wind in HO region.

The threshold of strong wind in the forecast model is defined as 14 m/s in this study by considering the model wind velocity represents the averaged wind speed in horizontal grid and integral period. The new method by using this threshold shows very good forecast performance of hit ratio of about 80%.

A performance of time series forecast every three hours was investigated. The forecast predicts longer gust wind period than the actual observation in the whole case. A potential of the precise time series forecast is intensively expected by adjusting the threshold.

This precise meteorological forecast system is based only on general purpose technology and does not adopt heuristics. Therefore, this forecast system is expected to be valid to the regional gust wind every part of the world.

Keywords: gust wind, MesoScale Model, dense observation, boundary layer

Development of high performance and low cost coherent doppler lidar.

YANO, Kenya^{1*} ; FURUMOTO, Jun-ichi¹ ; HIGASHI, Kuniaki¹ ; YABUKI, Masanori¹ ; HASHIGUCHI, Hiroyuki¹

¹Research Institute for Sustainable Humanosphere, Kyoto University.

In the summer season, the disastrous severe rain frequently occurs in Japan. The small-scale convergence of humidity in the boundary layer is considered as one of the most important factor to determine the generation of such a disastrous rainstorm.

Recently, the development of new metrological radar has been developing for monitor the rainstorm. It is, however, noteworthy that the result of the weather radar shows the echo from precipitation, which is falling down to ground in a couple of minutes. The forecast of rainstorm prior to 15-30 minutes is very difficult by using the weather radar only.

This paper develops the Coherent Doppler Lidar (CDL) to monitor the two-dimensional wind field in the atmospheric boundary layer. The new system improves the output power to increase the maximum height range. The high-performance and low-cost CDL will be realized by assembling the general fiber laser components, Dual polarization and multi-frequency observation is also included in the scope of this study to elucidate the characteristics of aerosol particles.

Keywords: Coherent Doppler Lidar, severe weather, Dual polarization, multi-frequency, aerosol

Temperature profiling with a rotational Raman lidar using a multispectral detector

OKATANI, Yoshikazu^{1*}; YOSHIKAWA, Kenichi¹; YABUKI, Masanori¹; TSUKAMOTO, Makoto²; HASEGAWA, Toshikazu²; TSUDA, Toshitaka¹

¹Research Institute for Sustainable Humanosphere (RISH), Kyoto University, ²EKO INSTRUMENTS CO., LTD.

Temperature profiling in the atmospheric boundary layer is essential for understanding atmospheric processes and for meteorological studies, such as precise weather forecasting with particular reference to heat-island phenomena, relative humidity retrievals, and transport characteristics of atmospheric pollutants in urban environments. Lidar has been considered one of the more powerful techniques for remote sensing of atmospheric parameters providing continuous observations with high spatiotemporal resolution. The temperature lidar method detects the temperature dependence of the intensities of the rotational Raman spectrum lines of atmospheric nitrogen and oxygen molecules. The polychromator design for conventional temperature lidar, which is much more complex than that for other lidar techniques, detects the ratio of two rotational Raman lidar signals of opposite temperature dependence using several edge and interference filters. In this study, we developed a temperature lidar with a multispectral detector (MSD), in order to construct a system that is compact, robust, and easy to align for the detection of rotational Raman signals. The multispectral detector enables simultaneous acquisition of multichannel photon counts and it provides spectral and range-resolved data by applying lidar techniques. The multispectral lidar detector can resolve the shape of the rotational Raman spectrum and therefore, temperature estimation can be accomplished by direct fitting of the observed lidar signals to the shape of the theoretical values of rotational Raman spectra that exhibit different dependencies on temperature.

To evaluate the accuracy of temperatures estimated by the proposed method, we constructed the temperature lidar, equipped with a 35-cm receiving telescope, with an MSD that has 0.34-nm spectral resolution at a laser wavelength of 355 nm. Two methods were considered for removing the leakage effects caused by strong elastic scattering in the detector. First, we covered one photomultiplier cathode strip of the elastic scattering channel to reduce crosstalk effects. Second, we blocked the major portion of elastic scattering from the polarization beam splitter using the polarization properties for spherical particles. Simultaneous measurements with the proposed rotational Raman lidar and radiosonde were conducted during January and February 2015 at the middle and upper (MU) radar observatory (34.8 N, 136.1 E) in Shigaraki, Japan. Here, we report the preliminary results of the temperature observations and the calibration process of the photon detection efficiency for each MSD channel.

Keywords: temperature lidar, multispectral detector